

COMPUTATIONAL AND EXPERIMENTAL MODELING OF SLURRY BUBBLE COLUMN REACTORS

Grant No. : DE-FG-98FT40117

US Department of Energy
National Energy Technology Laboratory
University Coal Research
Program Manager: Donald Krastman

TECHNICAL REPORT

Paul Lam, Principal Investigator
Associate Dean, College of Engineering
The University of Akron
Akron, OH 44326-3903
Tel. : 330-972-7230
Email : plam@uakron.edu

and

Dimitri Gidaspow, Co-Principal Investigator
Department of Chemical and Environmental Engineering
Illinois Institute of Technology
Chicago, IL 60616
Tel. : 312-567-3045 Fax : 312-567-8874
Email : gidaspow@iit.edu

August 2001

**COMPUTATIONAL AND EXPERIMENTAL MODELING OF
THREE-PHASE SLURRY-BUBBLE COLUMN REACTOR**

DE-FG-98FT40117

UCR

TECHNICAL REPORT

August 31, 2001

Professor Paul Lam, PI
College of Engineering
University of Akron
Akron, Ohio 44326-3901
Tel.: 330 972-7930
Fax 330 972-5162
E-mail: plam@uakron.edu

Professor Dimitri Gidaspow, Co-PI
Department of Chemical and
Environmental Engineering
Chicago, IL 60616
Tel.: 312-567-3045
Fax: 312 567-8874
Email gidaspow@iit.edu

Abstract

This project is a collaborative effort between the University of Akron, Illinois Institute of Technology and two industries: UOP and Energy International. The tasks involve the development of transient two and three dimensional computer codes for slurry bubble column reactors, optimization, comparison to data, and measurement of input parameters, such as the viscosity and restitution coefficients.

To understand turbulence, measurements were done in the riser with 530 micron glass beads using a PIV technique. This report summarizes the measurements and simulations completed as described in details in the attached paper, "Computational and Experimental Modeling of Three-Phase Slurry-Bubble Column Reactor." The Particle Image Velocimetry method described elsewhere (Gidaspow and Huilin, 1996) was used to measure the axial and tangential velocities of the particles. This method was modified with the use of a rotating colored transparent disk. The velocity distributions obtained with this method shows that the distribution is close to Maxwellian. From the velocity measurements the normal and the shear stresses were computed. Also with the use of the CCD camera a technique was developed to measure the solids volume fraction. The granular temperature profile follows the solids volume fraction profile. As predicted

by theory, the granular temperature is highest at the center of the tube. The normal stress in the direction of the flow is approximately 10 times larger than that in the tangential direction. The $\langle v'_z v'_z \rangle$ is lower at the center where the $\langle v'_q v'_q \rangle$ is higher at that point. The Reynolds shear stress was small, producing a restitution coefficient near unity. The normal Reynolds stress in the direction of flow is large due to the fact that it is produced by the large gradient of velocity in the direction of flow compared to the small gradient in the θ and r directions.

The kinetic theory gives values of viscosity that agree with our previous measurements (Gidaspow, Wu and Mostofi, 1999). The values of viscosity obtained from pressure drop minus weight of bed measurements agree at the center of the tube.

Measurement and Computation of Turbulence in Risers

Mehmet Tartan, Dimitri Gidaspow, Reza Mostofi, Yong Seop Shin

Department of Chemical and Environmental Engineering
Illinois Institute of Technology, Chicago, IL 60616
Fax: 312-567-8874, Email: gidaspow@iit.edu

The objective of this study is to understand turbulence in circulating fluidized beds (CFB). Tsuji, et al (1984) were the first to measure turbulent oscillations in gas-solid flow. Mudde, et al (1997) measured the turbulent stresses in a gas-liquid bubble column using PIV similar to that used here. Pan, et al (2000) used a hydrodynamic model to compute the Reynolds stresses for the data of Mudde, et al (2000). In the two-fluid approach, the use of averaged equations requires closure models. In order to improve multiphase models, such as described in Gidaspow's book (1994), a well-defined experiment is essential. Recently IIT CFB was rebuilt in order to correct the non-symmetrical behavior caused by the elbow type outlet. Figure 1 shows the schematic diagram of IIT CFB with a splash plate type outlet. The bed material was 530 micron glass beads with a density of 2.5 gr/cm³. The Particle Image Velocimetry method described elsewhere (Gidaspow and Huilin, 1996) was used to measure the axial and tangential velocities of the particles. Figure 2 shows a typical streak line generated on the computer screen. This method was modified with the use of a rotating colored transparent disk. The order of the colors on the streak lines indicates the direction of the flow. Figure 3 shows the velocity distributions obtained with this method. As can be seen in this figure the distribution is close to Maxwellian. From the velocity measurements the normal and the shear stresses were computed. Also with the use of the same CCD camera a technique was developed to measure the solids volume fraction. Figure 4 shows a typical picture used for this purpose. A probe was used in these experiments to obtain a radial profile of the measured values. Figure 5 shows the schematic diagram of the setup.

Figures 6 and 7 show the solids axial and tangential velocities profiles. The axial velocity profile is approximately parabolic and symmetrical. The tangential velocity was about 1/50 of the axial velocity, indicating a small rotational behavior that decreased close to the wall. The solids volume fraction profile is depicted in Figure 8. This figure shows that the riser is operating close to the core-annular regime. The solids volume fraction profile for 75 microns FCC particles (Miller and Gidaspow, 1992) shows a higher difference in the solids volume fraction between the core and annulus. The granular temperature profile is shown in Figure 9. This profile follows the solids volume fraction profile. As predicted by theory, the granular temperature is highest at the center of the tube. Figures 10 and 11 show the particle Normal and Reynolds stresses. The normal stress in the direction of the flow is approximately 10 times larger than that in the tangential direction. The $\langle v'_z v'_z \rangle$ is lower at the center where the $\langle v'_q v'_q \rangle$ is higher at that point. The Reynolds shear stress was small, producing a restitution coefficient near unity. The normal Reynolds stress in the direction of flow is large due to the fact that it is produced by the large gradient of velocity in the direction of flow compared to the small gradient in the θ and r directions.

The table summarizes the data and computation of viscosity using two methods. The kinetic theory gives values of viscosity that agree with our previous measurements (Gidaspow, Wu and Mostofi, 1999). The values of viscosity obtained from pressure drop minus weight of bed measurements agree at the center of

the tube. Particle velocities and concentrations were also measured as a function of time, as shown in Figures 13 and 14. Their principal frequency is almost one Hertz. See Fig 15 and 16. The variation of granular temperature with time is shown in Fig 17. The spectrum is in Fig18.

Preliminary computations, using model B in Gidaspow's book (1994) show a core-annular regime for the 530 microns glass beads with solids viscosity of $5.0 \times \epsilon_s$ as input. The computations are similar to those of Pan, et al using a CFDLIB code. The particle velocities are roughly the same as the experimental values. The velocity variances also follow the experimental trends but $\langle v'_z v'_z \rangle$ were much higher.

Acknowledgment

This study was supported by the National Science Foundation Fluid, Particulate and Hydraulic System Grant No. CTS-9610053, by the Department of Energy Grant No. DE-PS26-98FT40117 and by a gift from Dow Corning Corporation as a part of the Multiphase Fluid Dynamics Research Consortium.

References

- Gidaspow D. 1994, Multiphase flow and fluidization: Continuum and kinetic theory descriptions, Boston: Academic Press Inc.
- Gidaspow D. and Huilin L., 1996, Collisional viscosity of FCC particles in a CFB, *AIChE. J.* **42**, 2503-2510.
- Gidaspow D., Wu X. and Mostofi M., 1999, Turbulence of particles in a CFB and slurry bubble columns using kinetic theory, *AIChE annual meeting preprints*, Fluidization and Fluid-Particle systems, Dallas, 261-266.
- Miller A. and Gidaspow D., 1992, Dense, vertical gas-solid flow in a pipe, *AIChE. J.* **38**, 1801-1815.
- Mudde R.F., Lee J., Reese J. and Fan L.S., 1997, Role of coherent structures on Reynolds stresses in a 2-D bubble column, *AIChE. J.* **43**, 913.
- Pan Y., Dudukovic M.P. and Chang M., 2000, Numerical investigation of gas driven flow in 2-D bubble columns, *AIChE. J.* **46**, 434-449.
- Tsuji Y., Morikawa Y. and Shiomi H., 1984, LDV measurements of an air-solid two-phase flow in a vertical pipe, *J. Fluid Mech.* **139**, 417-434.

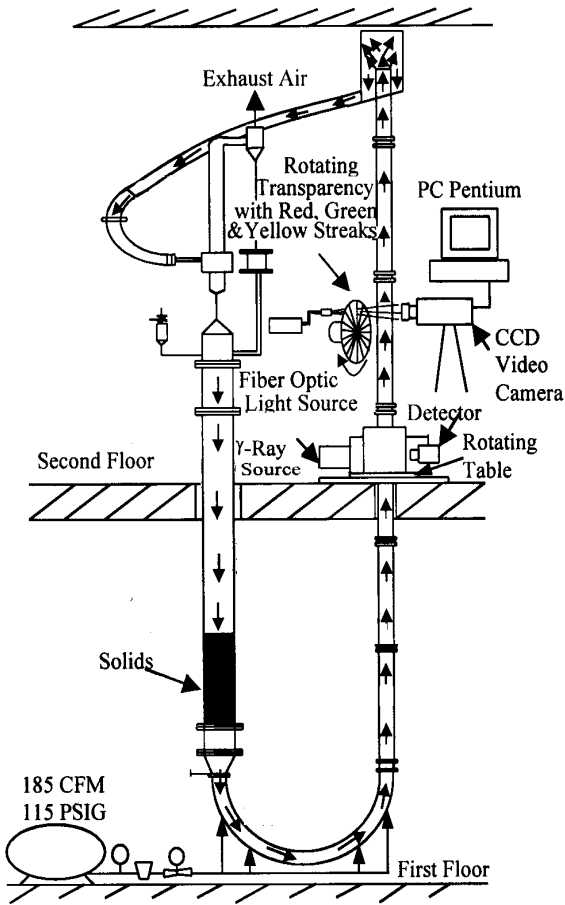


Fig. 1 IIT Circulating Fluidized Bed with Splash

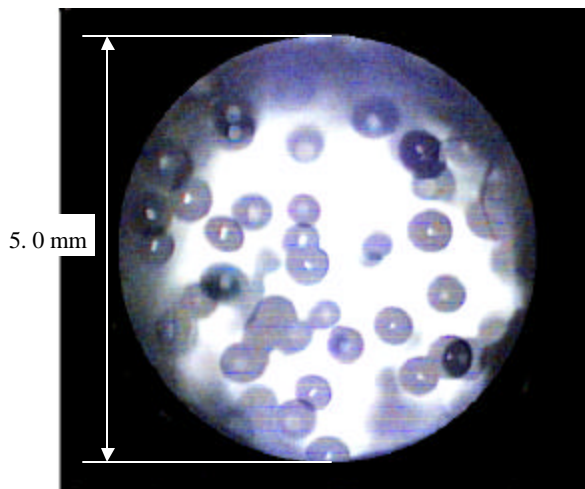


Fig. 4 Particle Image View Through CCD Camera

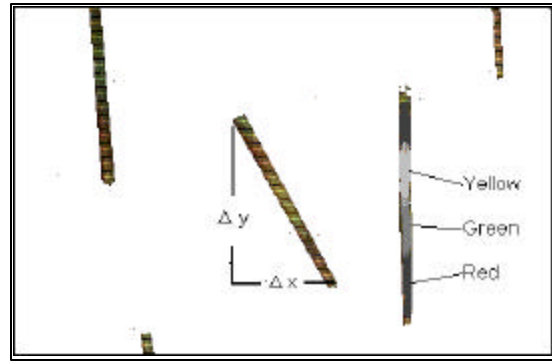


Fig. 2 Typical streak images captured by the

CCD camera, $d_p = 530 \mu\text{m}$
(Exposure time = 0.001s)

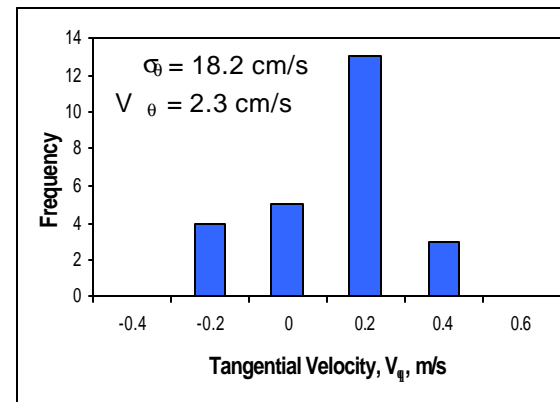
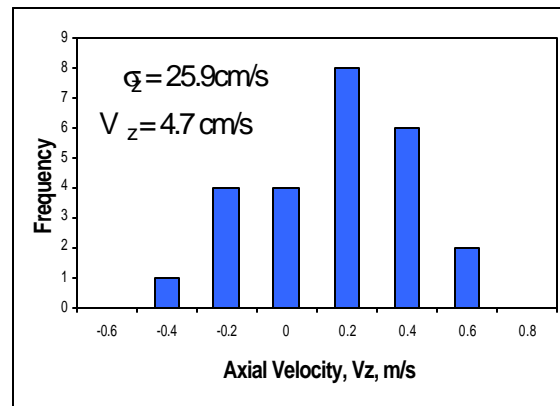


Fig. 3 Axial and Tangential Velocities, m/s, $d_p = 530 \mu\text{m}$,

$W_s = 14.6 \text{ kg/m}^2\text{s}$, $r_s = 2500 \text{ kg/m}^3$, $q = 444$

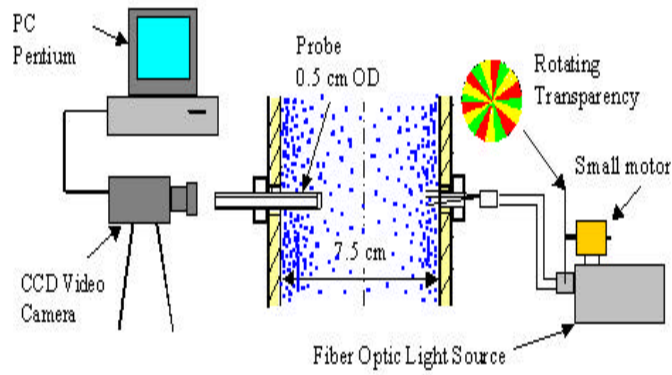


Fig.5 Particle Velocity and Solid Volume Fraction

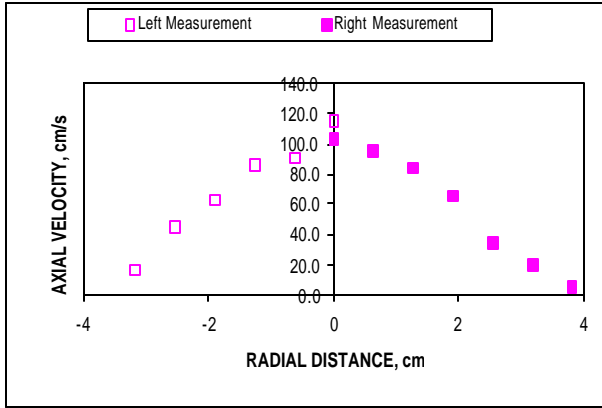


Fig.6 Particle Axial Velocity in the IIT Riser for 530 μm

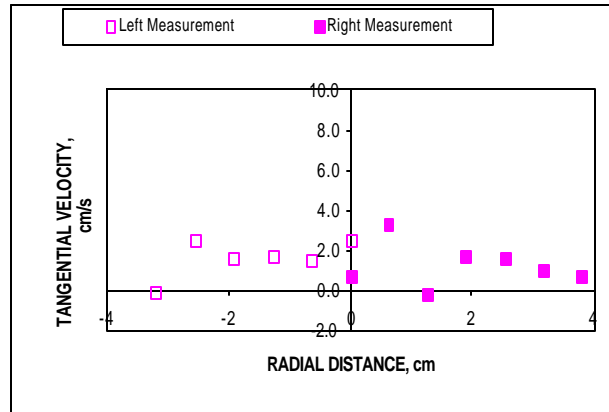


Fig.7 Particle Tangential Velocity

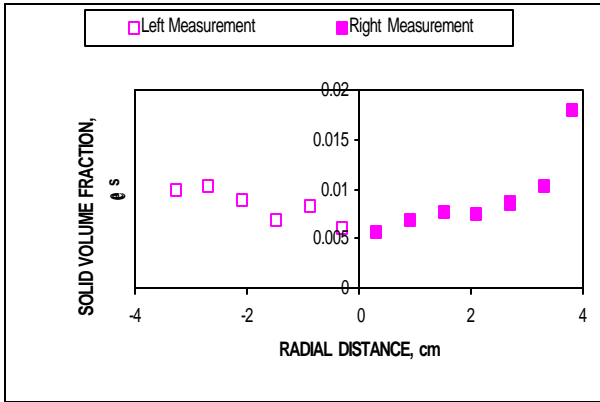


Fig.8 Particle Volume Fraction

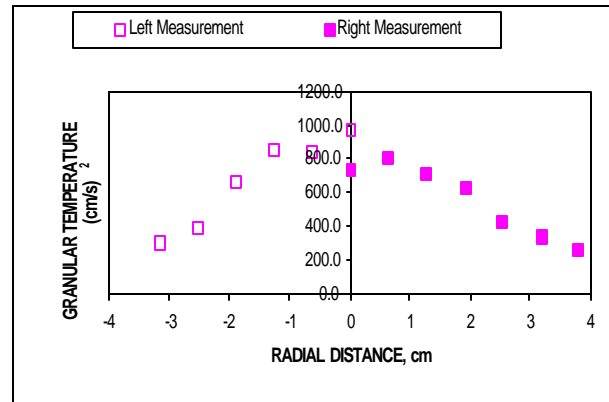


Fig.9 Granular Temperature in the IIT Riser for 530 μm

$$\text{Granular Temp., } q = \frac{2}{3} \sigma_{\theta}^2 + \frac{1}{3} \sigma_z^2$$

$$s_i^2 = \frac{1}{N} \sum_{i=1}^N (v_i - \bar{v})^2$$

$$\bar{v} = \text{Particle Average Velocity}$$

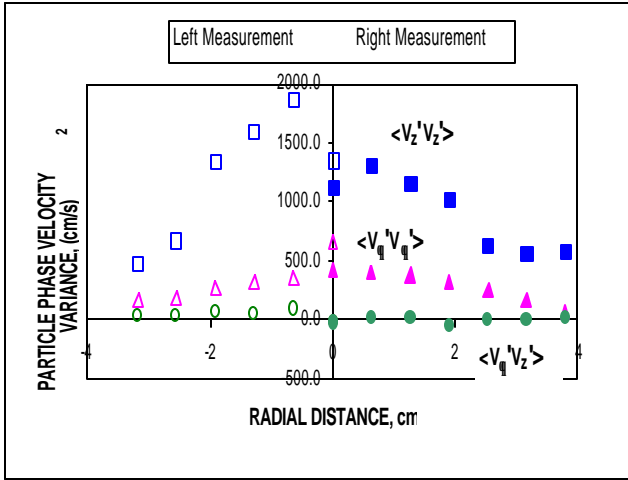


Fig. 10 Normal and Shear Reynolds Stresses

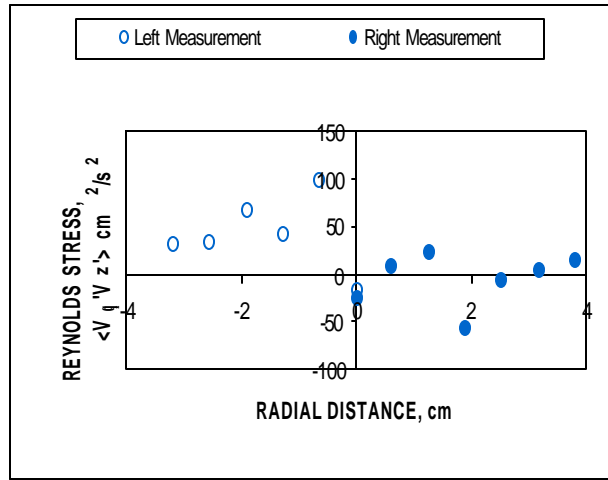


Fig. 11 Particle Phase Reynolds Stress

$$v_q'v_z' = \frac{1}{N} \sum_{i=1}^N (v_{q_i} - \bar{v}_q)(v_{z_i} - \bar{v}_z)$$

N = # of particles in a unit volume

$$\langle v_q'v_z' \rangle = \frac{1}{T} \int_0^T (v_q'v_z') dt$$

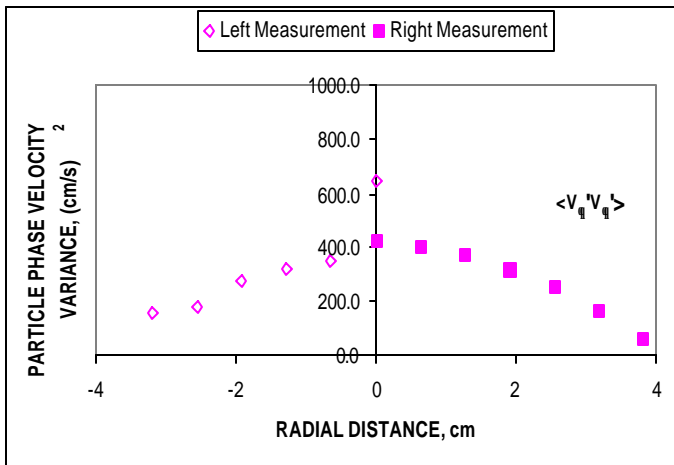


Fig. 12 Particle Phase Normal Reynolds Stresses

Solid Viscosity from Kinetic Theory:

$$m_s = \frac{5r_p d_p \sqrt{pq}}{48(1+e)g_o} \left[1 + \frac{4}{5}(1+e)g_o e_s \right]^2 + \frac{4}{5} e_s^2 r_p d_p g_o (1+e) \sqrt{\frac{q}{p}}$$

Viscosity from Mixture Momentum

Equation:

$$m = \frac{\left(-\frac{dP}{dz} \right) \frac{R}{2} - \frac{1}{R} \int_0^R \mathbf{e}_s \mathbf{r}_s g dr}{\left(-\frac{dV_s}{dr} \right)_{r=R}}$$

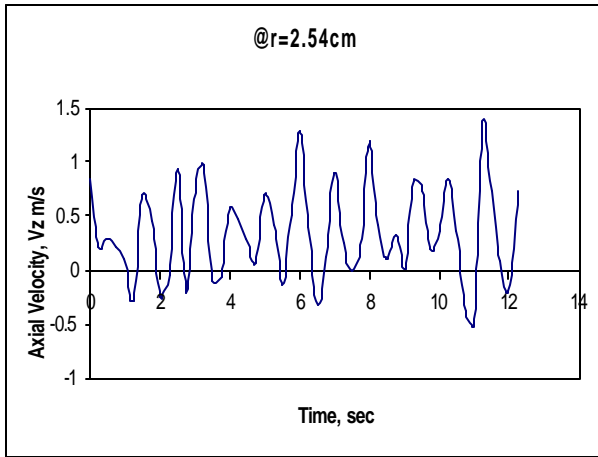


Fig. 13 Time Series of Solid Axial Velocity at

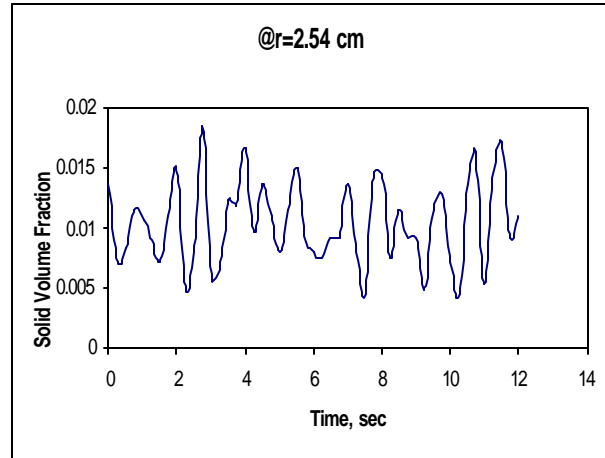


Fig. 14 Time Series of Solid Volume Fraction at $r=2.54\text{ cm}$

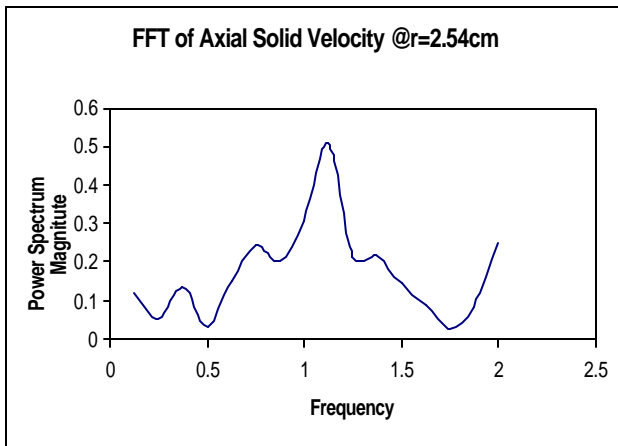


Fig. 15 FFT Analysis of Solid Axial Velocity at $r=2.54\text{ cm}$

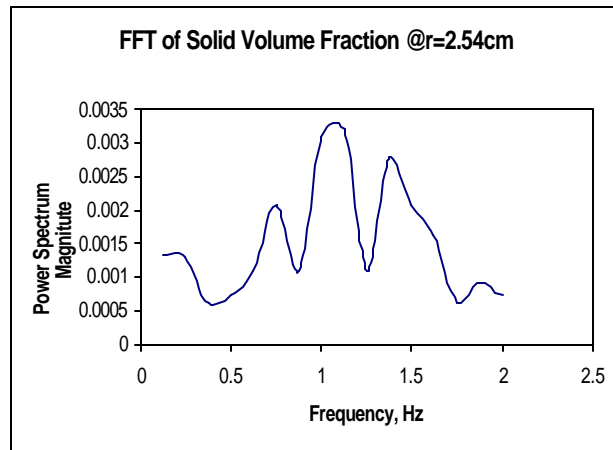


Fig. 16 FFT Analysis of Solid Volume Fraction at $r=2.54\text{ cm}$

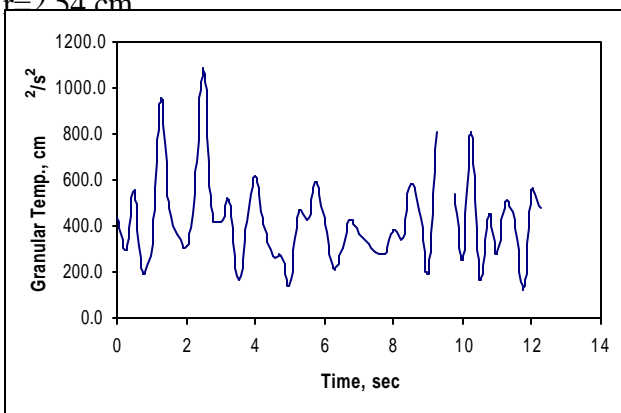


Fig. 17 Time Variation of Granular Temperature at $r=2.54\text{ cm}$

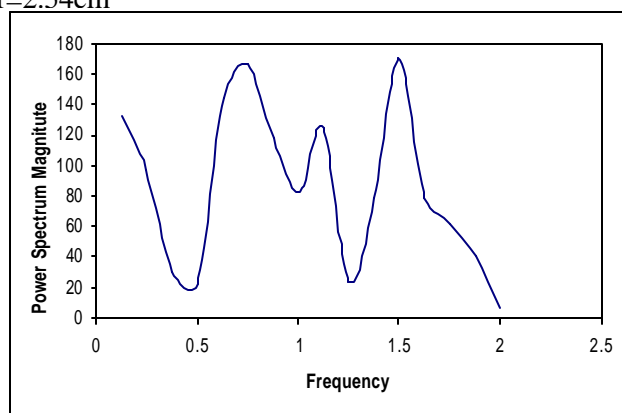


Fig. 18 FFT Analysis of Granular Temperature at $r=2.54\text{ cm}$